Complex Permittivity Measurement Method using a Reduced Uncertainty Mode-Matching Model for a Split-Cylinder Resonator

Master's thesis

January 2016

Maximilian Gattringer 0627822

3 Dielectric measurement methods at microwave frequencies

In the last chapter **??** we revisited the theory and physics of complex permittivity and we analysed the use of dielectrics in microwave engineering. While there is a true wealth of different dielectrics that are in use in microwave engineering, we decided to limit ourselves to low-loss dielectrics, such as substrates used in printed circuit board, insulators and dielectric resonators. Corresponding to the many varieties of dielectrics, there are just as many different methods for measuring the complex permittivity. At microwave frequencies (1-100GHz) we categorize the dielectric measurement methods into **travelling wave** methods and **standing-wave** methods, both of which bear 'wave' in their name reflecting the wave nature of the electromagnetic waves at microwave frequencies.

3.1 Travelling-wave methods

Travelling-wave methods use the scattering parameters of a measurement cell to directly determine the dielectric properties of a specimen. Waves are emitted into the measurement cell and the response in the form of transmitted and reflected waves, is measured. The waves typically travel through a waveguide or free-field medium in the measurement cell and interact with the specimen while they pass through. They enter the measurement cell through one or multiple ports, which may or may not have the same reference impedance. ~~If each port has the same reference impedance, they enter the cell undisturbed and propagate in the cell~~. From the solution of the field equations in the measurement cell, the field configuration of the waves is already given. When the wave meets the specimen in the measurement cell the wave is reflected by the transition from the measurement cell medium into the specimen medium. One part of the wave is reflected at this first boundary, another part can transmit through the boundary and propagate in the medium. Depending on the composition of the measurement cell one or multiple boundaries can exist in a cell, which in turn can cause multiple transmission and reflection events. Using suitable models for the measurement cell, we can derive the properties of the specimen. Typically we would like to determine the permittivity $\epsilon = \epsilon' - j\epsilon''$ and the permeability $\mu = \mu' - j\mu''$ of the speci[illegible]. Like the permittivity the permeability ~~also~~ depends on the frequency, the orientation of the field in the measurement cell, the temperature and the composition of the specimen. While the temperature and composition of a specimen is typically known and is therefore included in the model, the anisotropy of each property is generally not known. To simplify the matters here the specimens can be assumed to be isotropic. Such simplifications limit the number of different specimen types that can be measured, but the approach is acceptable as many technically relevant dielectrics are isotropic. This limits the number of unknowns in the measurement to two (ϵ, μ), which can be solved using the results of a transmission and reflection measurement (S_{11}, S_{12}, S_{21} and S_{22}). As a result the permittivity and the permeability of a specimen can be derived simultaneously in a transmission and reflection measurement.[1, 2]

The decisive advantage of travelling wave methods over standing wave methods is that the measurement frequency can be chosen freely and is not determined by the measurement cell. This allows us to use travelling-wave methods over a very wide range of frequencies as long as the model that we use in our measurements is valid. Another advantage is simplicity, if we assume for example that we only want to measure non-magnetic dielectrics we can use a complex reflection coefficient measurement to measure the complex permittivity of a non-magnetic specimen over a wide frequency range. The downside of travelling wave methods is that we use the results of our scattering parameter measurements directly. While this allows us to perform broadband measurements, it limits the accuracy that we can achieve using this method. This is not so much a problem when we measure the real part of the complex permittivity, but rather when we try to measure the loss tangent. The magnitude of the loss tangent varies very strongly with the type of dielectric. Medium to high-loss dielectrics can have a loss tangent of above one and low-loss dielectrics can have one of around 5×10^{-5}~~, less than a ten thousandth of the value of the other type!~~ A wave transmitted through a thin, low-loss specimen is barely attenuated by the specimen. The sensitivity of travelling-wave methods for these low-loss specimens is therefore relatively low, and noise and other loss processes also drive up the uncertainty of the method.

3.2 Standing-wave methods

Since travelling-wave methods are not able to measure low-loss specimens accurately, we continue this discussion of dielectric measurement methods with the method that lies in the focus of this thesis - the standing-wave or resonance method. The fundamental idea behind the standing-wave method is that the measurement cell is a microwave resonator, which resonates with the specimen inside the measurement cell. Usually the resonant frequency f_r of the measurement cell determines the dielectric constant of the specimen and the quality factor Q the loss tangent. Unlike the travelling-wave method the standing-wave method only measures the complex permittivity at the resonant frequencies of its resonances, so the results lie at discrete frequencies and are not broadband. Although the method delivers far less frequency points, the results of each measurement can be very accurate if implemented correctly. With this qualitative advantage standing-wave methods are usually the most accurate methods for

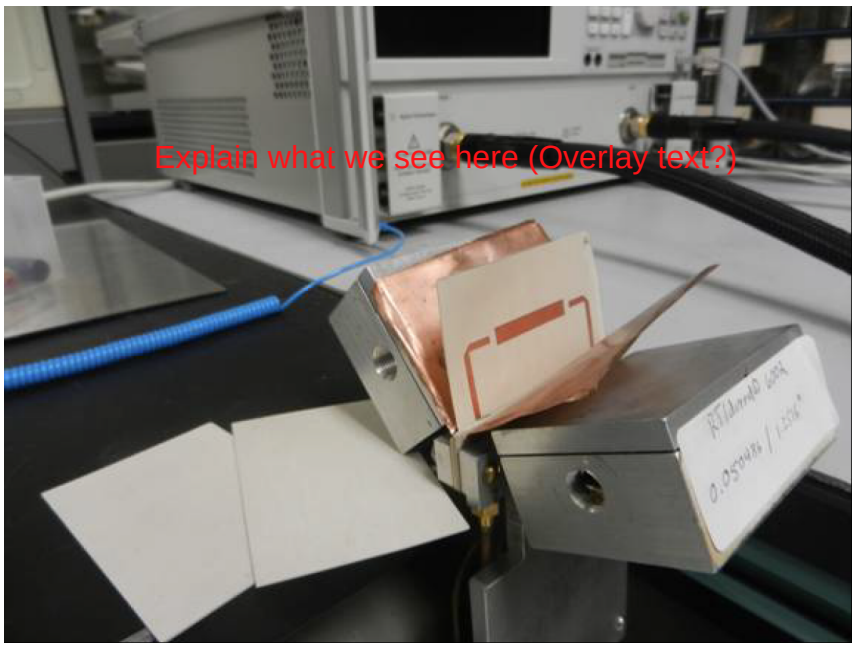

Figure 1: Stripline resonator according to IPC TM-650 2.5.5.5c, photograph taken from [3]

low-loss materials. The measurement cells can be chosen as such that they provide higher field strengths in the specimen for some measurement modes, which increases the loss in the specimen and therefore also the sensitivity of loss measurements. Still, both measurement methods have their merits: For example, a disadvantage of the standing-wave method is that these methods can usually only handle non-magnetic specimens. This makes it very attractive to use a combination of both methods. A non-resonant method is used to get a general knowledge of the electromagnetic properties over a wide frequency range. A resonant method is used to get accurate measurements at discrete frequencies.

Many different variants of the standing-wave method exist, at lower resonant frequencies ~~many~~ microwave cavities are used. Cavities are metallic enclosures around a dielectric field region, which can be used as microwave resonators. If the specimen itself is cut to a certain shape and excited by a suitable coupling network, the measurement set-up becomes a dielectric resonator. This dielectric resonator can then be used for dielectric measurement, for example for dielectric bricks used in dielectric resonators. At millimetre wave frequencies (30GHz and above) wave techniques are used very often, since cavities at these frequencies become increasingly small. All techniques have in common that they require suitable models to compute the complex permittivity from a measured resonance. Many methods use analytical or numerical models of the resonator and the specimen to achieve this. Another approach is the resonant perturbation technique, which has been very popular before the advent of computational electro-magnetics. Resonant perturbation typically means that a small specimen is inserted into a cavity with very well known fields inside it. The fields are disturbed by the specimen, but the influence of the specimen is so low that it does not change the fields inside the cavity very strongly. In such case the original solution for the cavity can be used with a simple perturbation term to measure the permittivity of the specimen.

~~To give the reader a deeper understanding of the standing-wave method,~~ we are now going to introduce three different standing-wave methods. Firstly, we will introduce the planar circuit methods, which are especially popular among printed circuit board manufacturers and circuit designers. We will explain why these methods are usually not the best choice for low-loss specimens and why other methods are usually superior in performance compared to these methods. Secondly, we give a brief introduction into the Split-post dielectric resonator, which is one of the most accurate methods for low-loss dielectrics in the 1-10GHz frequency range. It is also very similar to the method that is the topic this thesis, the Split-cylinder resonator, which we will discuss in Chapter **??**. Lastly, we will introduce a quasi-optical technique, the open-resonator method, to give the reader an insight into how dielectric measurements are performed at millimetre-wave frequencies.

3.3 Planar circuit methods

Substrate and printed circuit board manufacturers often perform dielectric measurements, which are very important for the quality control in printed circuit board manufacturing and for the design of electronic circuits. The reason for this is that high-frequency electronics manufacturers need a consistent ϵ_r value for their production, which

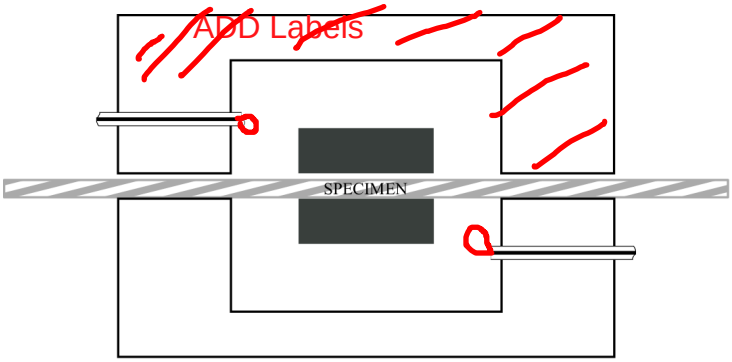

Figure 2: Split-post dielectric resonator.

implies a tight ϵ_r control in PCB production. The ϵ_r of a substrate must not vary more than 0.5% from batch-to-batch and within the sheet itself. To measure these small variations in the dielectric substrates a measurement method with an accuracy of less than 0.5% must chosen.[3] As manufacturers are well experienced with printed circuit techniques, many of them use printed circuits for their dielectric measurement. Typically, they use one of the popular planar transmission lines like striplines, microstrips or co-planar transmission lines. These can be used in travelling-wave methods or standing-wave methods for planar circuits, but we will only discuss the standing-wave methods here as the former suffer from the same issues as other travelling-wave methods. Widely used standing-wave techniques are ring resonators, T resonator and strip line resonators. Especially the "clamped stripline" resonator of IPC standard IPC-TM-650 2.5.5.5c [4] is widely used by PCB manufacturers and measurement results can be found in many datasheets. The method is illustrated in Fig. 1, two pieces of unclad substrate are sandwiched together with a thin strip of copper and two coupling strips in the middle, and are then pressed together by two pieces of copper at the top and the bottom. The result is a capacitively coupled strip line resonator, which allows quick and repeatable dielectric measurements that are excellent for quality control.

Planar circuit techniques have very genuine advantages, first of all the field orientation of the electric field in the substrate is the same as in a real circuit. As single-ended planar transmission lines have one or multiple ground planes, the field orientation in the material is mostly perpendicular to the surface of the material. Combined with the fact that most PCB materials are mildly anisotropic, a measurement method that has the same field orientation as a circuit delivers the right dielectric constant for that circuit. Secondly, planar substrate techniques can include all loss mechanisms in a circuit - dielectric losses and conductor losses. As there are various types of copper claddings available on the market, measuring both loss mechanisms can deliver better predictions for the performance of a circuit as the entire system of copper cladding and dielectric is measured and not only the dielectric. For a PCB manufacturer these two are very important advantages, but these advantages pose serious challenges for dielectric measurements. In case of the field orientation, the orientation of planar circuits is not only perpendicular to the substrate, but there are also fringing fields that have field components parallel to the surface. The influence of fringing fields depends on the type of transmission line. Microstrips, for example, have far stronger fringing fields than strip lines, which can cause measurement errors in anisotropic materials. This makes microstrip resonators and transmission lines far less suitable for dielectric measurements. Another disadvantage of the perpendicular field orientation are air gaps that cause systematic measurement errors, understating the dielectric constants of high-ϵ_r laminates.

For the loss measurements the situation is not much better, if we wanted to measure the dielectric losses of a material, we would have to separate the dielectric losses from the total losses in the material. As the conductor losses are typically far higher, there is a large uncertainty for the dielectric losses in the material. This makes substrate methods far less attractive for low-loss dielectrics. For example, according to NIST Technical Note 1520[5] the ring resonator and the T resonator are limited to materials with a loss tangent $\tan\delta > 1 \times 10^{-3}$. Additionally the results of open structures like microstrip lines or co-planar strip lines may be affected by radiation losses. Impurities introduced by the manufacturing of the copper cladding may also change the dielectric properties. All in all, planar circuit methods are interesting options for approximate dielectric measurements of cladded printed circuit board substrates, since they offer the right field orientation in the substrate and they include most loss mechanisms in the material. For accurate dielectric measurements they should be used with utmost care, since systematic errors like airgaps, field orientation, anisotropy and conductor losses can negatively affect a measurement.

3.4 Split-post dielectric resonator method

The second standing wave method that we would like to discuss here, the Split Post Dielectric Resonator method, bears many similarities to the Split-Cylinder method and other TE_{0n} mode cavities. It was developed by Krupka, Nishikawa and DelaBalle in the 1980s and is one of the easiest and most convenient methods for measuring dielectric properties. It has become an industry standard for the measurement of PCB laminates and dielectric substrates.[6] Figure 2 illustrates the geometry of a Split Post Dielectric resonator. The resonator consists of two cylindrical microwave cavities that both have a dielectric resonator placed along the z-axis of the cavity. One half is placed above the other with a small gap still separating the two halves. The resonator is then excited by coupling loops inserted into the bottom cavity and the top cavity. When the resonator is excited, the two dielectric bricks in the cavity experience a coupled $TE_{01\delta}$ resonance and the two resonators are coupled by evanescent fields. Unlike the evanescent fields of a single resonator, the evanescent fields between the two dielectric resonators are relatively strong. Dielectric specimens can therefore be placed in the gap between the two cavities and perturb the resonance of the resonator. Again, we can use the perturbation of the resonator to measure the complex permittivity of the specimen.[1, 7, 8]

Since most of the electro-magnetic energy is stored in the dielectric resonators and in the region between the two resonators, there is far less interaction with the cavity walls than in a typical cavity method. This allows the Split Post to have a far greater sensitivity for dielectric loss measurements and resolutions as low as 2×10^{-5} for $\tan\delta$ may be achieved. Split Posts can be manufactured in a frequency range from 1 to 36GHz, but they only operate at a single frequency. Their advantage over other cavity methods is that the frequency shifts of Split Posts are generally smaller and that the measurement frequencies for different specimens are roughly the same - a cavity may be detuned by a specimen as much as 3GHz! Like TE_{0n} mode cavities, the evanescent field is also circularly polarised and therefore continuous across air-dielectric interfaces. This mitigates the influence of airgaps and allows the operator to measure thin films and coatings.[1, 7, 8]

Although the resonator has many advantages, there are a few downsides: First of all, the modelling of the Split Post is far more complicated than other dielectric measurement methods. There are no analytical models, so numerical techniques like Mode-matching, finite-difference, finite-element or Rayleigh-Ritz methods must be employed. Although it is very similar to perturbation methods, it cannot be modelled using perturbation methods. Secondly, their are restrictions on the thickness of the specimens. ~~Specimens~~ can only be as thick as to allow strong coupling between the two resonators. At higher frequencies decoupling ~~can occur very early and~~ even thinner specimens may be required. Lastly, the technique is not usable at millimetre frequencies and becomes increasingly hard to use ~~for frequencies over~~ 10GHz. At these frequencies cavities have to be very small and the thickness of the specimens is very limited, so Split Post Dielectric resonators are typically used from 1-10GHz. Overall, the Split Post Dielectric resonator method is an excellent method for measuring thin, low-loss dielectrics in the 1-10Ghz frequency range. The dielectric constant of thin specimens can be measured with an accuracy of less than $\pm 0.3\%$ and the resolution of the loss tangent measurements may be as small as 2×10^{-5}, although these figures may be worse for thicker specimens.[1, 7, 8]

3.5 Open-resonator methods

At millimetre wave frequencies many methods become increasingly hard to use, cavities for example become inconveniently small as their sizes are usually proportional to the wavelength λ. At these frequencies quasi-optical techniques like the open resonator method are used very often. An open resonator is a microwave Fabry-Perot interferometer, which uses two mirrors to focus electromagnetic waves in between these ~~two~~ mirrors. A specimen is then placed between the ~~two~~ mirrors and, like for all other standing wave methods, the quality factor and the resonant frequency of the cavity are ~~then~~ used to measure the complex permittivity of a specimen at the resonant frequency. Different variants of the method exist and they can measure specimens over a wide frequency range 10-200GHz. According to NPL[1] it is one of the most accurate and important methods for low-loss dielectrics at millimetre-wave frequencies. It allows measuring the dielectric constant with an uncertainty of $\pm 0.2\%$ for $\epsilon_r < 3$, $\pm 1\%$ for $\epsilon_r \approx 50$ and the loss tangent with an uncertainty of $\pm 10\%$ for $\tan\delta > 2 \times 10^{-4}$. The measurement modes of the cavity are TEM_{00n} Gaussian beam modes, so the electromagnetic waves in the cavity are focussed to a beam like in an optical resonator. The field orientation of the electric field varies over the beam length, so the placement of a specimen along the beam length would influence the measurement. To circumvent this, the sample is typically placed at the beam waist, where the field is nearly linearly polarised. ~~Depending on the geometry of the resonator the beam waist may be halfway between the two mirrors, like for the symmetric resonator shown in Fig. 3, or somewhere else between the two mirrors. At the beam waist the method measures the in plane permittivity of a specimen in a single direction.~~ This allows the open resonator method to measure in-plane anisotropy of a specimen just by rotating the specimen in the beam.[1, 2]

Compared to other methods, the method has a few very unique advantages. First of all, like any free field

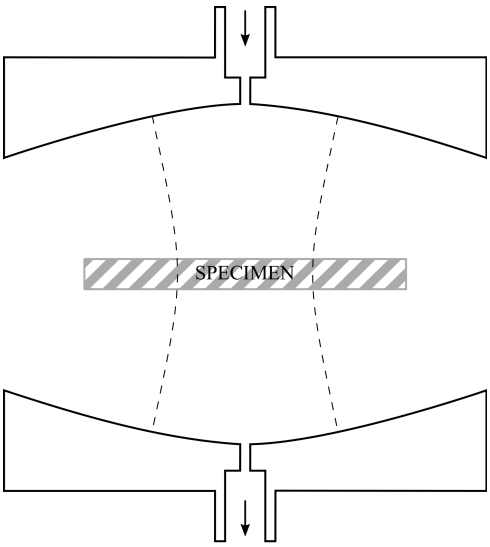

Figure 3: Open resonator with two concave mirrors coupled to waveguides, adapted from [1].

method it allows easy insertion and removal of specimens, which do not have to be machined into certain shapes like for the measurements in a cavity. Typically, large laminar specimens are used that are large enough to encompass the whole cross-section of the Gaussian beam. As the beam width depends on the frequency different specimens sizes are required at different frequencies. At 10GHz, for example, specimens can be as large as 200mm, whereas at 72GHz a specimen may be as small as 35mm. Apart from the size, specimens should be reasonably flat and composite materials should be checked for high-ϵ_r filling materials as these can cause an scattering error in the measurement. Certainly, frequencies far lower than 10Ghz are less attractive for the open resonator method and at these frequencies microwave cavities are usually preferred. Another advantage of the method are the high quality factors of its resonances, which are about 60,000 at 10GHz and can reach 200,000 at 100GHz and above. Together with a far less densely populated resonance spectrum, typical issues of microwave cavities like mode-coincidence and mode-interference are far less common. The quality factor of cavities on the other hand is proportional to $\lambda^{3/2}$, since losses increase with higher frequencies. Specimen losses grow slowly, so the sensitivity of cavity methods falls with higher frequencies. Higher modes in cavities have higher quality factors, but the number of modes grows with frequency and mode interference becomes an issue. This is also an essential advantage of open resonators, while the number of modes in an open resonator is proportional to the length $\frac{L}{\lambda}$, it is proportional to the volume $\left(\frac{L}{\lambda}\right)^3$ in cavities. Open resonators can be large, but the mode separation is still far better than in comparable cavities. All things considered, the open resonator method is a very versatile standing wave method, which can accurately measure the complex permittivity at microwave frequencies. The large frequency range, the ability to measure the anisotropy of a specimen and its good mode separation make it indispensable measurement method.[1, 2]

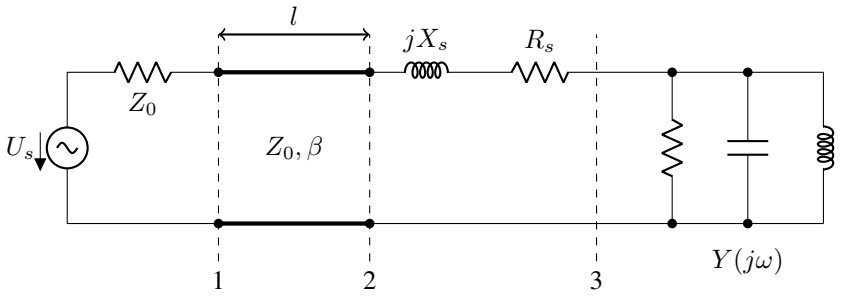

Figure 4: A simple RLC circuit

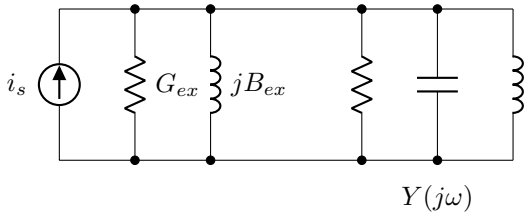

Figure 5: Thevenin equivalent circuit of Fig.4, shunt impedances shown in eq.(4)

4 Quality factor measurements - An introduction

As we have mentioned before resonant permittivity measurements use the resonances in an RF resonator to determine the complex permittivity of a specimen. Depending on the number of degrees of freedom in the resonator, one or multiple resonances may exist. Typically an RF resonator has multiple resonances, also called modes, which are also the degrees of freedom of the system. To model the resonances in an RF resonator we can use a simple RLC circuit, which has only one degree of freedom to describe more complicated systems.

Fig. 4 shows an example of such a simple RLC circuit. An AC source with source impedance Z_0 feeds a simple RLC circuit through a transmission line of length l and impedance Z_0. Depending on the coupling mechanism a lossy inductor may be used to model the coupling.

$$f_0 = \frac{1}{2\pi\sqrt{LC}} \qquad Q_0 = \frac{2\pi f_0 C}{G_0} \tag{1}$$

By coupling we understand the flow of power in and out of the resonator when it is excited by a source. A simple RLC circuit is capable of oscillating on its own, but to measure the properties of the resonance we need to excite the resonator and measure its response. This measurement "loads" the resonator, i.e. the power lost in the measurement increases the loss of the resonator. Therefore, we characterise a resonator through its resonant frequency f_0 and its unloaded quality factor Q_0, in case of the RLC circuit this is shown in equation (1). The quality factor is a measure for the loss in a resonator and determines how fast the energy oscillating in the resonator will be lost. As can be seen in equation (2) the quality factor Q is proportional to the average energy $\overline{W}$ divided by the losses P in a resonator. This ratio is also a time constant for the energy $W(t)$ oscillating in the resonator at an angular frequency $\omega_0 = 2\pi f_0$.

$$Q = \frac{\omega_0 \overline{W}}{P} \qquad W(t) = \overline{W} e^{-t/\tau} \qquad \tau = \frac{Q}{\omega_0} \tag{2}$$

In case of the RLC circuit in Fig. 4 the lossy inductive coupling loads the resonator, the loaded resonator has a resonant frequency f_L and a loaded quality factor Q_L that is different from the unloaded resonator. Using the Thevenin equivalent circuit of Fig. 5 it can be shown that the loading of the resonator depends on the Thevenin shunt impedances.

Using a convienient expression for the admittance of the RLC circuit,

$$Y(\omega) = G + j\omega C + \frac{1}{j\omega L} = G + j\sqrt{\frac{C}{L}}\left(\frac{f}{f_0} - \frac{f_0}{f}\right) = G(1 + jQ_0\delta) \tag{3}$$

introducing a detuning factor,

$$\delta(f) = \frac{f}{f_0} - \frac{f_0}{f} \qquad \delta(f) = 0 \Leftrightarrow f = f_0 \tag{4}$$

we yield an expressions for f_L and Q_L of the loaded resonator.

$$B_{ex} + G_0 Q_0 \delta_L = 0 \Rightarrow \delta_L(f_L) = \frac{-B_{ex}}{G_0 Q_0} \qquad Q_L = \frac{\omega C}{G} = \frac{\omega_L C}{G_0 + G_{ex}} \tag{5}$$

We used the resonance condition $\mathrm{Im}(Z) = 0$ for linear lumped circuits, i.e. voltage and current in the resonator are in phase. From a physical point of view this means that the electrical energy is equal to the magnetic energy in the circuit. This condition also is also satisfied by the electro-magnetic field in a cavity at resonance.

$$i_s = \frac{U_s}{R_s + Z_0 + jX_s} \qquad G_{ex} = \frac{R_s + Z_0}{(R_s + Z_0)^2 + X_s^2} \qquad B_{ex} = \frac{X_s}{(R_s + Z_0)^2 + X_s^2} \tag{6}$$

Due to the fact that the coupling only detunes a resonator lightly, we can use the first-order Taylor series

$$f(\delta) \approx f_0(1 + \delta/2) \Rightarrow f_L \approx f_0(1 + \delta_L/2) = f_0(1 - \frac{B_{ex}}{2G_0 Q_0}) \tag{7}$$

to describe the detuning of the resonator. If the coupling is sufficiently small or mostly resistive, we can derive a simplified expression for Q_L and introduce a coupling coefficient κ to model the coupling of such a resonator.

$$Q_L = \frac{\omega_L C}{G_0 + G_{ex}} \approx \frac{\omega_0 C}{G_0 + G_{ex}} = Q_0 \frac{1}{1 + \frac{G_{ex}}{G_0}} = Q_0 \frac{1}{1 + \kappa} \tag{8}$$

With this simple example of an RF resonator we have now introduced the concepts of resonant frequencies and quality factors of loaded and unloaded resonators. Although real RF resonators have multiple resonances, the concepts introduced here can be used to characterise each mode of a real resonator. For complex permittivity measurements we are interested in the properties of the unloaded resonator, since the coupling is usually only a mean to couple energy in and out of the resonator. In many cases the real part of the permittivity is derived from the unloaded resonant frequency and the imaginary part is derived from the unloaded quality factor.

For the complex permittivity measurements it is vital to accurately measure these resonances. This is achieved by accurate measurements of the reflection coefficient or the transmission coefficient at ports of the resonator with vector network analysers (VNA) or similar devices. A resonator may have one or multiple ports through which measurements can be performed. Irrespective of the number of ports, measurements using the reflection coefficient are reflection-type measurements and measurements using the transmission coefficient are transmission-type measurements.

4.1 Reflection-type measurements

An example for a reflection-type measurement is shown in Fig. 4. The ideal voltage source U_s with its internal resistance Z_0 is a representation of a reflection coefficient measurement, where the reflection coefficient is measured at reference plane (1). In Fig. 6 the Smith chart of this reflection-type measurement is illustrated. Beginning at reference plane (3) a shunt RLC circuit draws a circle on the Smith chart over frequency, where the resonant frequency is the location on the Smith chart with the smallest reflection coefficient, marked with a cross on the Smith chart. If we assume that the series resistance R_s is small, the reflection coefficient is transformed mainly by the inductive coupling of the resonator. In reference plane (2) the reflection coefficient is rotated in a clockwise direction and its diameter is changed. As we have discussed previously, this changes the resonant frequency and the quality factor of the resonator. The resonant frequency at reference plane (2) is marked by a triangle and lies right next to the original resonant frequency of the RLC circuit, which is still marked by a cross. The resonant frequency at reference plane (2) lies also at the point with the smallest reflection coefficient. For the quality factor we can see that the coupling increases the loaded quality factor a little bit over the situation at reference plane (3), where the reference impedance led to a critically coupled resonator. Finally, the transmission line rotates the resonance circle while we move from reference plane 2 to reference plane 1. This rotation has no influence on the measurement of a resonance circle if the bandwidth of the resonance is narrow, i.e. the quality factor is high, and can be compensated by an appropriate counter-rotation.

While it is possible to find the point of resonance on a Smith chart, the Smith chart does not show the frequency of the resonator at resonance. It is more convenient to take the frequency sweep over the complex reflection coefficient like in Fig. 7 and use appropriate techniques like the 3dB method to find the resonant frequency and quality factor of the resonator. We will elaborate on these techniques in this chapter. The magnitude of the reflection coefficient plot has a characteristic bell shape that reaches a minimum at the resonant frequency (again marked by an x in the plot) and the width of the bell is a measure for the quality factor of the resonator. This is the characteristic behaviour that can be observed for every resonator around its resonant frequency. We can show

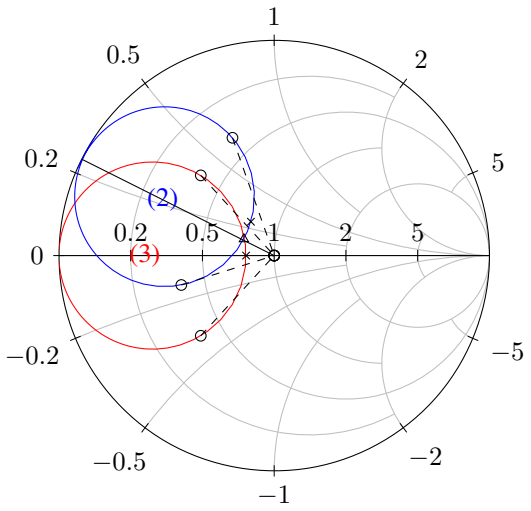

Figure 6: Smith chart of a reflection-type measurement

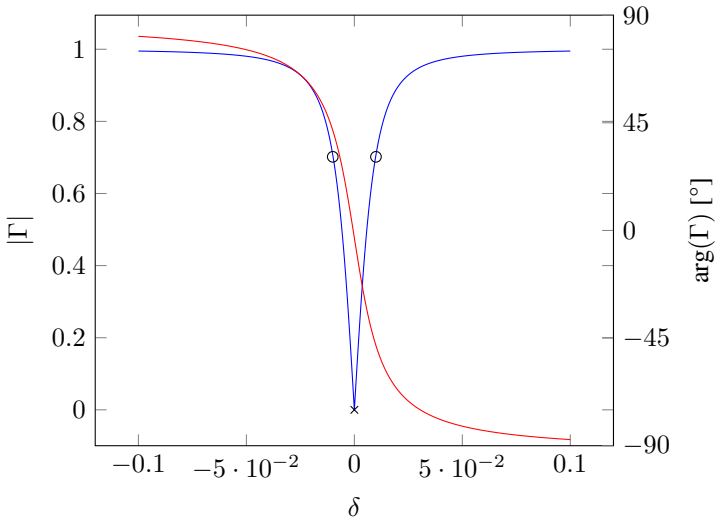

Figure 7: Reflection coefficient of a critically coupled resonator plotted over the detuning factor δ.

that a shunt RLC circuit has a similarly shaped reflection coefficient for any network that has a sufficiently flat frequency response around the resonant frequency of the RLC circuit. For an arbitrary two-port with admittance matrix Y driven by a source with source impedance Z_0, we can show for the reflection coefficient of a shunt RLC circuit at the input of the two-port:

$$\Gamma(\delta) = \frac{Y_0 - Y_{11}}{Y_0 + Y_{11}} + \frac{2Y_0 Y_{21} Y_{12}}{(Y_0 + Y_{11})^2 (G_{in} + G)(1 + jQ_L(\delta + \frac{B_{in}}{GQ_0}))}. \tag{9}$$

The reflectometer draws a circle on the Smith chart due to the expression $1 + jQ\delta$ in the denominator. The circle begins for large negatives values of δ in its origin at $\frac{Y_0 - Y_{11}}{Y_0 + Y_{11}}$ on the Smith chart, runs down to the resonance point at $\delta = \delta_L = -\frac{B_{in}}{GQ_0}$ and returns to its origin for large δ. For our example in Fig. 4 the expression simplifies to

$$\Gamma(\delta) = \frac{R_s + j\omega L_s - Z_0}{R_s + j\omega L_s + Z_0} + \frac{2Z_0}{(Z_0 + R_s + \omega L_s)^2 (G_{ex} + G)(1 + jQ_L(\delta + \frac{B_{ex}}{GQ_0}))}, \tag{10}$$

which is the analytical solution of Fig. 6.

4.2 Transmission-type measurements

As we discussed previously the second method of quality factor measurement methods uses the transmission coefficient to measure the resonances of a cavity. In Fig. 8 an example for a transmission-type measurement

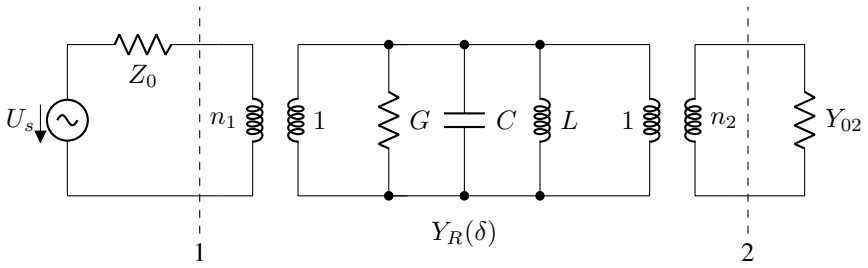

Figure 8: Example for a resonator with two coupling networks

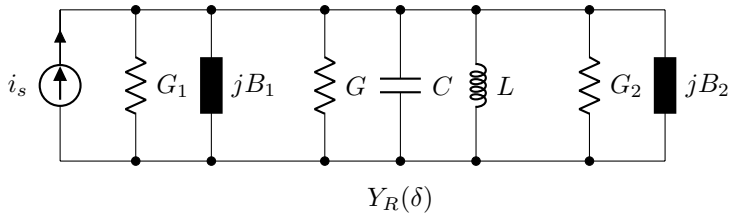

Figure 9: Norton equivalent circuit of Fig. 8

is shown, in this example the transmission coefficient S_{21} is measured between reference plane 1 and reference plane 2. This time the resonator is coupled to two ports through two ideal transformers, which as we will find out later are convenient models for coupling loops. These two coupling networks now both load the resonator, so the additional loss introduced by the coupling networks now stems from both ports. The same thing happens to the reactive loading, which now detunes the resonator from both ports. When we take a look at Fig. 9 we can see that the shunt admittances are transformed into the resonator, where

$$Y_1 = n_1^2 Y_{01} = G_1 + jB_1 \qquad Y_2 = n_2^2 Y_{02} = G_2 + jB_2 \tag{11}$$

are the results of this transformation.

Like in Fig. 5 we can use the resonance condition $\mathrm{Im}(Y) = 0$ to calculate the loaded resonant frequency f_L, where δ_L is the detuning factor at the loaded resonant frequency. For the loaded quality factor in equation (13) we can use the definition for the quality factor to do the same, where a light reactive loading assumption allows us to introduce coupling factors κ_1 and κ_2 for port 1 and port 2.

$$B_1 + B_2 + G_0 Q_0 \delta_L = 0 \Rightarrow \delta_L(f_L) = -\frac{B_1 + B_2}{G_0 Q_0} \tag{12}$$

$$Q_L = \frac{\omega_L C}{G + G_1 + G_2} \approx \frac{\omega_0 C}{G + G_1 + G_2} = Q_0 \frac{1}{1 + \frac{G_1}{G} + \frac{G_2}{G}} = Q_0 \frac{1}{1 + \kappa_1 + \kappa_2} \tag{13}$$

For the transmission coefficient the situation is again very similar. To simplify the matters here we assume that the load and source admittance are both real, i.e. conductances. A meaningful assumption, since the load and source impedances in most of our measurements are more or less conductances as well.

$$S_{21} = \frac{2\sqrt{n_1^2 Y_{01} n_2^2 Y_{02}}}{n_1^2 Y_{01} + n_2^2 Y_{02} + G(1 + jQ_0\delta)} = \frac{2\sqrt{n_1^2 Y_{01} n_2^2 Y_{02}}}{(n_1^2 Y_{01} + n_2^2 Y_{02} + G)(1 + jQ_L\delta)} \tag{14}$$

$$\kappa_1 = \frac{n_1^2 Y_{01}}{G} \qquad \kappa_2 = \frac{n_2^2 Y_{02}}{G} \tag{15}$$

Having a $(1 + jQ\delta)$ factor in the denominator as well equation (14) proves that the transmission coefficient also draws a circle in the complex plane. Like for the reflection coefficient this behaviour is not limited to real reference admittances, but - as we will prove in the appendix - this applies also to the transmission coefficient of any resonator.

4.3 Resonance curve measurements

We have now discussed the two fundamental types of resonance measurements. As we have seen, the reflection coefficient and transmission coefficient of both measurement configurations are very similar. Both draw circles in

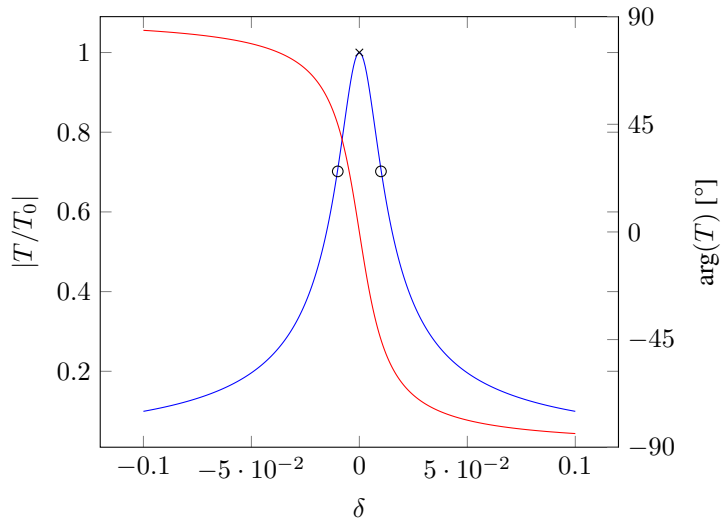

Figure 10: Typical resonance curve - Transmission coefficient of a undercoupled resonator plotted over the detuning factor δ.

the complex plane due to the $(1 + jQ_0\delta)$ factor in their frequency response. This bell-shaped frequency response is characteristic for any resonance in linear circuits. Due to this, the frequency response over the magnitude and the phase is typically used to measure the resonances in a system. Different techniques are used to estimate the quality factor Q and the resonant frequency ω_r from measured frequency responses, which in turn can be used to calculate the unloaded quality factor Q_0 and the unloaded resonant frequency ω_0 if the coupling coefficients of the resonator are known. Most of the algorithms used to estimate the properties of a resonator are fitting techniques that fit the measurements to a known objective function. The parameters of such fits are typically the properties of the resonator or are used to calculate the properties.

The most well-known of these methods - a method that everyone is familiar with - is the **3dB method**. A simple method, which estimate the resonant frequency from the maximum of the magnitude and the quality factor from the 3dB bandwidth of the curve. It assumes an undisturbed resonance curve

$$g(\omega) = \frac{g_0}{\sqrt{1 + Q^2(\frac{\omega}{\omega_0} + \frac{\omega_0}{\omega})^2}}, \tag{16}$$

which naturally has its peak magnitude $g(\omega = \omega_0) = g_0$ at the resonant frequency ω_0. If we take the half-power points of the 3dB bandwidth we find the quality factor as follows,

$$\frac{g_0}{2} = \frac{g_0}{\sqrt{1 + Q^2(\frac{\omega_{3dB}}{\omega_0} + \frac{\omega_0}{\omega_{3dB}})^2}} \qquad Q = \frac{f_0}{2\Delta f}\left(\frac{1 + \frac{\Delta f}{f_0}}{1 + \frac{\Delta f}{2f_0}}\right) \underset{f_0 \gg 2\Delta f}{\approx} \frac{f_0}{2\Delta f}. \tag{17}$$

Obviously, we can approximate the quality factor using this simple formula, if the resonant frequency f_r is much smaller than the bandwidth $2\Delta f$. This is a very useful results and it can be used to estimate the properties of resonance curves. Unfortunately, it is not the most accurate method, since only two or three points of the curve are actually used in the measurement. Today, when we measure resonance curves using a network analyser we measure many more points, so a lot of the available information is not used in the measurement. If the data is noisy the results of the measurement will be very inaccurate.

Overdetermined measurement methods can use more points and are therefore usually more accurate. These methods are typically computer-based and use linear least-squares or non-linear least-squares fitting algorithms. As the frequency response is a complex function, the magnitude and phase of the function can be fitted. Algorithms that also fit the phase are circle-fits. All algorithms use the same complex objective function

$$g(\omega) = \frac{g_0}{1 + jQ(\frac{\omega}{\omega_0} + \frac{\omega_0}{\omega})}, \tag{18}$$

which must be adapted to the measurement. The adaptations compensate for the offset due to coupling, the phase shift on the transmission line, noise and other parasitic influences. Often this is achieved through adding up a suitable polynomial to the objective function.

Petersan and Anlage [9] compared the accuracy and precision of seven different methods and used both complex data and magnitude data for their comparison. The performance of the methods was compared for different signal-to-noise ratio (SNR) and quality factor values. They found that the most precise methods use complex data for their fits and use weights in their fits to give noisy data less weight. The phase vs. frequency method - a circle-fit variant - was the most accurate and most precise method for higher SNR values in their comparison. At the same time a magnitude fit - the Lorentzian fit [10]- was the most robust method and provided good results even for very low SNR values. The Lorentzian fit used a Cauchy-Lorentz probability distribution function as approximation to the resonance curve, where a Taylor series was used for the detuning factor to calculate the approximation. Their results (Table 1) also indicate that both methods outperform the 3dB method in terms of accuracy.

Method	$Q = 10^3$		$Q = 10^5$		Power ramp (SNR$\approx 1 - 2000$)	
Type	Q	f_0	Q	f_0	Q	f_0
3dB	3.29×10^{-2}	1.71×10^{-5}	3.36×10^{-2}	1.71×10^{-7}	12.49	6.41×10^{-8}
Lorentzian	2.00×10^{-3}	2.18×10^{-6}	2.09×10^{-3}	2.52×10^{-8}	$\mathbf{3.11 \times 10^{-2}}$	$\mathbf{1.46 \times 10^{-9}}$
Phase vs. freq.	$\mathbf{1.3 \times 10^{-4}}$	$\mathbf{7.88 \times 10^{-8}}$	$\mathbf{1.4 \times 10^{-4}}$	$\mathbf{1.46 \times 10^{-9}}$	1.25×10^{-1}	1.75×10^{-8}

Table 1: Relative accuracy of 3dB method, Lorentzian method and Phase vs. Freq. method for two values of quality factors and over different SNR values. Best value in each column is written in bold. Adapted from Petersan and Anlage[9].

Although Petersan and Anlage give a very good overview over the different methods used, we would like to mention two more methods that were previously used for the Split-Cylinder resonator. The first method is the **Coakley method** developed by researchers at the NIST [11]. The method, which has strong similarities to the Lorentzian fit, was also used for the measurements in Dr. Janezic's PhD thesis [12]. It is a weighted non-linear least-squares technique that uses only the magnitude of the frequency response. Since the convergence of NLLS fits is better for good initial values, the method first approximates the resonant frequency and quality factor using a LS squares method (Estin's method [13]), then an initial NLLS fit is made using the objective function

$$T(f) = \frac{T(f_0)}{1 + Q^2(\frac{f}{f_0} - \frac{f_0}{f})^2} + BG. \tag{19}$$

Next, the residuals of this fit are squared and put in different equidistant frequency bins, these binned residuals are then used as weights in the final weighted non-linear least squares fit, which yields the resonant frequency and quality factor of the measurement. Being a robust method like the Lorentzian fit, the Coakley method was definitely developed with noisy data of undercoupled resonators in mind.

The second method we would like to mention is the **Bartley-Begley circle-fit** [14], a modified version of the phase vs. frequency method that is used for the quality factor measurements in the Keysight split-cylinder software. The objective function was merely adjusted to make it suitable for undercoupled resonators,

$$T(f) = L + \frac{de^{-2jd}}{1 + jQ\left(2\frac{f - f_0}{f_0}\right)}. \tag{20}$$

The function was linearised, a complex leakage term and a phase rotation term were added.

4.4 Coupling and measurement resonators - Which method is best?

While resonators are employed in different kinds of applications like filters or oscillators, the purpose of resonators in complex permittivity measurements is different from these applications. As we only need the properties of the unloaded resonator we are not interested transferring high power through the resonator. In the last paragraphs we learned that the amount of power coupled in and out of the resonator depends on the coupling coefficient. Depending on the coupling coefficient we know three types of coupling:

$$\begin{array}{cc} \text{Under-coupled} & \kappa < 1 \\ \text{Critically-coupled} & \kappa = 1 \\ \text{Over-coupled} & \kappa > 1 \end{array}$$

High-power applications like filters and oscillators are mostly critically coupled or over-coupled, since they want to dissipate more power in the circuitry rather than in the resonator. Of course, one could argue that if we knew the coupling coefficient, measuring with higher power would be better, since we could measure the reflection coefficient or the transmission coefficient with a higher SNR. Unfortunately, measuring the coupling coefficient

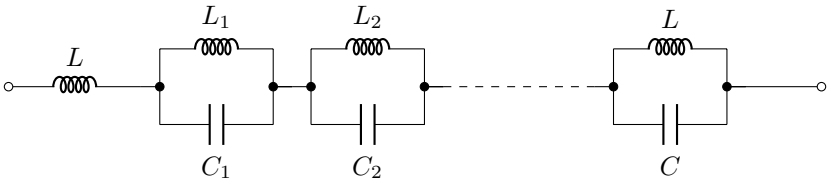

Figure 11: Foster's equivalent circuit of a lossless one-port

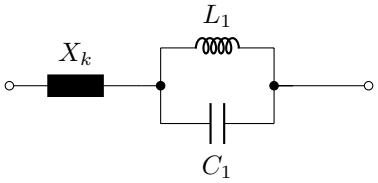

Figure 12: Equivalent circuit of a single mode

introduces a great amount of uncertainty as well, since the coupling coefficient is frequency-dependant and is also different for each mode of a cavity. It might be possible to measure κ for each mode, but to circumvent the problem altogether we can choose to under-couple the resonator. That means we reduce the coupling for each port so much that $Q_L \approx Q_0$ and $\kappa \approx 0$. This eliminates the influence of the coupling on the quality factor and can - depending on the type of coupling - also reduce the influence on the resonant frequency. Under-coupled resonators are logical choice for measurement resonators like ours, but the small coupling coefficient can also increase the input impedance of the resonator. This can, as we will see when we discuss the coupling of our resonator, make reflection coefficient measurements very inaccurate, since the accuracy of reflectometers close to the unit circle in the Smith chart is very low.

4.5 Resonance phenomena and microwave cavities

At the beginning of this chapter we have mentioned that a series or a parallel resonant circuit can be used to model the resonances of a cavity. We have extensively used RLC circuits in this chapter to explain the concepts of quality factor measurements and to show how different measurement methods work. Up to now we have not given any explanation why RLC circuits can be used to model single modes in a cavity.

To prove this we will use a variant of Foster's theorem for distributed circuits, of which waveguides and cavities are prominent examples. Foster's theorem - originally formulated for lumped circuits - states that any lossless, n-mesh circuit with a pair of terminals has an impedance function, which in turn can be represented with n LC circuits in parallel or n LC circuits in series. The theorem has also been shown to apply to distributed circuits as well. If we calculate the input impedance of an arbitrary, lossless one-port with respect to the mean stored magnetic and electric energy in the one-port, we yield equation (21) for the input impedance.

$$Z(j\omega) = \frac{j\omega 2(W_H - W_E)}{\frac{1}{2}ii^*} \tag{21}$$

The frequencies for which $W_H = W_E$ are the poles and zeros of equation (21) and are also the resonant frequencies of the one-port. Using Foster's theorem, $Z(j\omega)$ can be expanded into the series

$$Z(j\omega) = j\alpha_1\omega - 2\sum_{n=1}^{\infty} r_n \frac{j\omega}{\omega^2 - \omega_n^2}, \tag{22}$$

where α_1 and r_n are positive constants, and ω_n are the resonant frequencies of the one-port. As shown in Fig. 11, this expansion can be represented by an inductor an infinite number of LC circuits in series.

At frequencies close to the resonant frequency of an LC circuit, i.e close to a pole, the influence of all the other modes diminishes and the value of the impedance is dominated by this LC circuit. Of course, this is only the case if all other resonant frequencies are far away from the resonant frequency of the dominant resonance. In an equivalent circuit (Fig. 12) the influence of all the other modes is combined to an nearly-constant term X_k and a single LC circuit with resonant frequency ω_n.

Until now, we have discussed the situation for lossless circuits, which already illustrates how the impedance of an arbitrary distributed circuit can be described by the poles of the circuit. Although this may be true for lossless

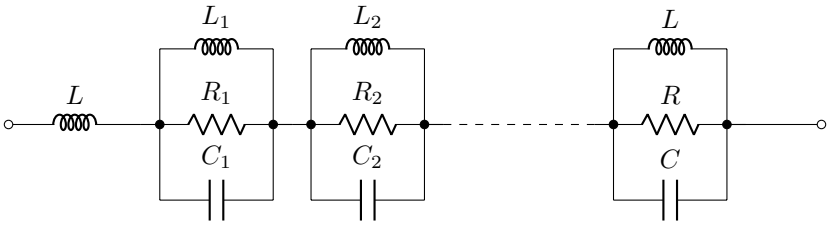

Figure 13: Foster's equivalent circuit of a microwave cavity

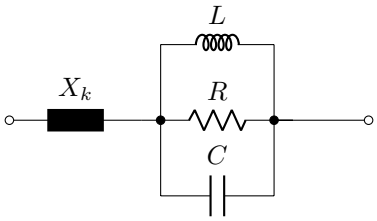

Figure 14: Equivalent circuit of a single mode of a cavity

circuits, we have ignored that every real circuit is lossy. For slightly lossy circuits it has been shown that Foster's theorem applies as well. The derivation for this theorem is similar to the derivation in the lossless case, only this time a complex frequency $\lambda = j\omega + \xi$ is used in the derivation. Interestingly, the theorem breaks down for higher losses, but applies to distributed circuits with low loss. A condition that is conveniently fulfilled by any meaningful cavity. Foster's theorem for slightly lossy distributed circuits shows that any low-loss cavity can be expanded in an infinite number of resonant circuits, where the resonant frequencies of the cavity are the resonant frequencies of the resonant circuits. The equivalent circuit of a cavity developed from the input impedance of a circuit is shown in Fig. 13 and uses an inductor and lossy parallel resonant circuits for each resonant frequency. A similar development exists for the admittance of a circuit and uses lossy series resonant circuits. This equivalent circuit (Fig. 13) brings us back to the original question we had, how a single resonant circuit can represent a cavity. Again, if we calculate the impedance around a resonant frequency f_r and if all other resonant frequencies lie far away, a single resonance dominates and the contribution for all other modes are so small that they can be modelled by a constant term X_k. Clearly, a single mode can be represented by a single resonant circuit and a constant impedance X_k, although the constant term is ignored in many instances to simplify the matters even more. (Fig. 14)

Similar developments exist for multiple terminals as well and we have reasons to believe that resonant circuits are a meaningful way to model the modes in any cavity. The model is still an approximation and it is only valid, if all the other resonant frequencies are far away. If another resonance lies very close to the resonance we want to measure, we would need another resonant circuit for our model to model the interference by another resonance. In many cavities the distances between modes shrink with higher frequencies and there are even cases where so-called degenerate modes have identical resonant frequencies. The Split-Cylinder resonator is a cylindrical cavity that has certain degenerate TM and TE modes. It is still possible to measure each of these modes, as we have conveniently left out the influence of coupling in these derivations. The terminals we spoke of in connection with equation (21) were not defined in any way, we can choose them according to our needs, which leads to our next topic, the coupling of cavities.

4.6 Coupling of cavities

As we have discussed previously, coupling networks are used to couple energy in and out of a resonant circuit and the degree of coupling is described by the coupling coefficient κ. In case of a cavity the terminals of the cavity are the terminals of the coupling networks that connect the cavity to the circuit. Due to the properties of this coupling network, each mode has its own coupling coefficient κ_n, which is defined by how the coupling network interacts with the mode fields in the cavity. This interaction is achieved by either inserting parts of the coupling network into the volume of the cavity or by attaching them to the boundaries of the cavity. Unlike in the case of the resonant circuit, the coupling of a cavity does not only load the resonator, but it also changes the modes inside the resonator. Owing to this mode perturbation a field calculation must include the coupling networks. Unfortunately, only a few special field problems have simple, analytic solutions, while most problems can only be solved using numerical computations. To avoid these issues coupling networks are often designed as such that they try to disturb the fields inside the cavity as little as possible to approximate the fields with the undisturbed solution. If a coupling network

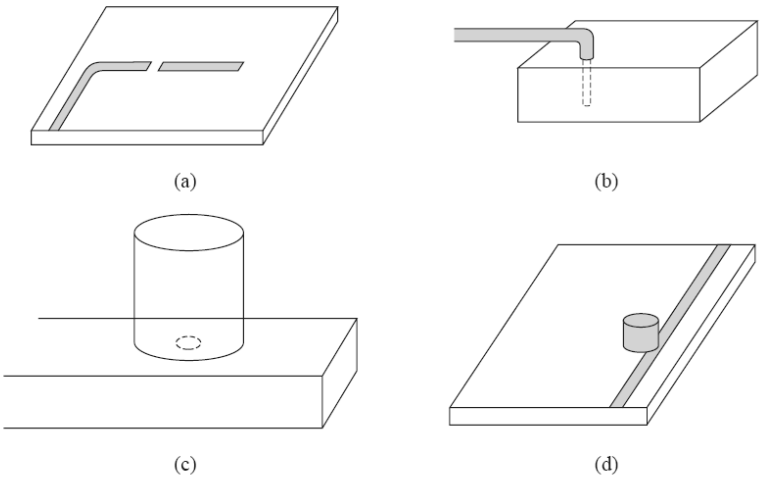

Figure 15: Coupling to mircrowave resonators. From Pozar - Microwave Engineering. [15]

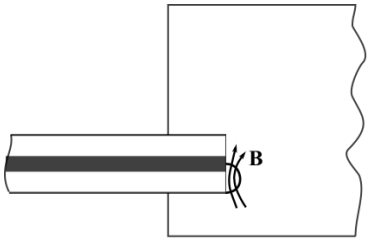

Figure 16: Coupling loop

disturbs the fields in a cavity only very little, its coupling coefficient will also be relatively small. A convenient result, since we have already stated that a small coupling coefficient is a good choice for a measurement resonator.

In Fig. 15 a few examples for couplings to microwave resonators are shown. Coupling networks usually cater to certain feed lines, modes or desired reactive loads. Fig. 15a shows a gap-coupled microstrip resonator, which couples capacitively from a microstrip to a microstrip resonator. Fig. 15b features an electric probe coupling that couples between a coaxial line and a rectangular waveguide cavity. These two examples were both for (Quasi-)TEM lines, but Fig. 15c exemplifies a rectangular waveguide as feed line and a simple hole in the waveguide as coupling to a cylindrical cavity attached to the waveguide. Finally, Fig. 15d shows a microstrip coupling to a dielectric resonator. Obviously, there is a wide number of different couplings for microwave resonators, for the Split-Cylinder resonator we have chosen to use magnetic loop coupling (Fig. 16). Magnetic loop coupling uses a coaxial line as feed line, which is inserted into the cavity and has the inner conductor connected to either the walls of the cavity or the outer conductor of the feed line. Due to this loop an incident wave creates a loop current in the cavity, which acts more or less like an electrically small magnetic loop antenna.

Using a Lagrangian method an equivalent circuit (Fig. 17) for small loops with an approximately constant loop current can be found. The equivalent circuit shows that every mode in the cavity is inductively coupled to the input of the loop by a mutual inductance M_{0n}. Equation (23) states that each orthonormal mode $\mathcal{H}_n$ in the cavity with magnetic flux lines running through the loop is coupled out of the cavity. The strength of this coupling depends on the flux running through the loop $\int \vec{B} \cdot \vec{n} dA$, the permeability of the field region inside the cavity μ and the wave number $k_n = \omega_{0n}\sqrt{\epsilon\mu}$.

$$M_{0n} = \mu k_{0,n} \int_{\mathcal{A}} (\vec{n} \cdot \vec{\mathcal{H}}) dA \qquad \frac{1}{V} \int_{\mathcal{V}} (\vec{\mathcal{H}_n} \cdot \vec{\mathcal{H}_m}) dV = \delta_{m,n} \tag{23}$$

The other circuit elements of each resonant circuit are defined by the resonant frequency $\omega_{0n} = \frac{1}{\sqrt{L_n C_n}}$ and the quality factor of the mode $Q_n = \frac{\omega_{0n} L_n}{R_n}$, finally the self-inductance of the coupling loop is modelled by the inductor L_0. Regarding the mutual inductance it is interesting to note that the wave number and the permeability are non-zero constants, while the flux through the loop depends on the location and the orientation of coupling

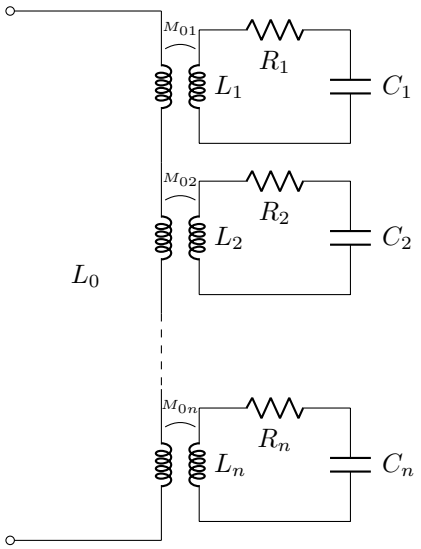

Figure 17: Equivalent circuit of a magnetic coupling loop according to [16]

loop in the magnetic field. This can be used to amplify or suppress certain modes in a cavity by either locating the coupling loop in an area with a relatively strong field or by turning the loop into the direction of a strong field component. A very useful property, which as we will see in our discussion of the Split-Cylinder resonator, allows us to separate the transverse magnetic and transverse electric fields of a cavity.

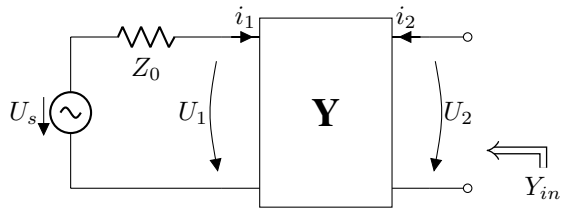

Figure 18: Input resistance of a two-port coupling network

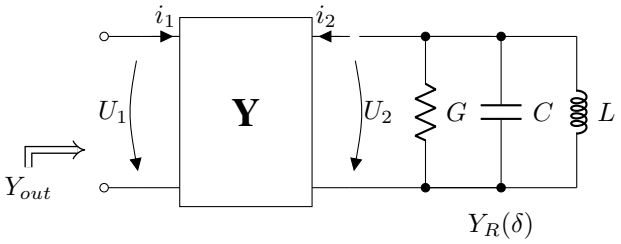

Figure 19: Input resistance of a two-port coupling network

A Reflection coefficient of a coupled resonant circuit

In section 4 we have discussed the reflection-type measurement of resonant circuits, where we provided an expression for the reflection coefficient of a resonator with arbitrary coupling. The coupling was modelled using an admittance matrix Y, which can serve as a model for an arbitrary two-port. Since we did not find this expression anywhere else in the literature, we decided to add it to this treatise. It is a very convenient expression, which allows us to prove that the reflection coefficient of any resonator is shaped similarly, independent of the coupling network.

To derive this expression, we calculate the input admittance of an arbitrary two-port shown in Fig. 18, which is fed by an ideal voltage source with source impedance Z_0. The input admittance Y_{in} equals

$$Y_{in} = Y_{22} - \frac{Y_{21}Y_{12}}{Y_{11}+Y_0} = G_{in} + jB_{in}, \quad Y = \begin{pmatrix} Y_{11} & Y_{12} \\ Y_{21} & Y_{22} \end{pmatrix} \tag{24}$$

where $Y_0 = 1/Z_0$ is the source admittance of the source and Y is the admittance matrix of the coupling network.

To calculate the reflection coefficient, we measure the output admittance on port one. For the measurement we remove the circuitry on port one and add a shunt RLC circuit on port two. (Fig. 19) As previously mentioned the shunt RLC circuit is a model for a single mode of a microwave cavity, which can be shown using the Foster theorem. The admittance of the RLC circuit is $Y_R = G(1 + jQ_0\delta)$, where $\delta(f) = \frac{f}{f_0} - \frac{f_0}{f}$ is again the detuning factor and $Q_0 = \omega L/C$ is the unloaded quality factor of the circuit. The output impedance is

$$Y_{out} = Y_{11} - \frac{Y_{12}Y_{21}}{Y_{22}+Y_R}. \tag{25}$$

With the output impedance at hand, we can calculate the reflection coefficient for a reference admittance $Y_0 = 1/Z_0$.

$$\Gamma = \frac{Y_0 - Y_{out}}{Y_0 + Y_{out}} = \frac{Y_0 - Y_{11}}{Y_0 + Y_{11}} + \frac{2Y_0Y_{12}Y_{21}}{(Y_0+Y_{11})^2(Y_{in}+Y_R)} \tag{26}$$

Equation (18) was used to simplify the expression. When we further insert the admittances Y_R and Y_{in}, and introduce a loaded quality factor $Q_L = Q_0/(1 + G_{in}/G)$, we yield:

$$\Gamma = \frac{Y_0 - Y_{11}}{Y_0 + Y_{11}} + \frac{2Y_0Y_{12}Y_{21}}{(Y_0+Y_{11})^2(G_{in}+jB_{in}+G(1+jQ_0\delta))} \tag{27}$$

$$= \frac{Y_0 - Y_{11}}{Y_0 + Y_{11}} + \frac{2Y_0Y_{12}Y_{21}}{(Y_0+Y_{11})^2(G_{in}+G)(1+jQ_L(\delta+\frac{B_{in}}{GQ_0}))} \tag{28}$$

If we look for the resonance term in the reflection coefficient of eq. (28), we can see that the resonance term $1+jQ_L\delta$ lies in the denominator. All the other factors of the equation are either add up or divided by the resonance. Since we know that many resonances have a very narrow band, we can safely assume for many coupling networks that the resonance dominates the frequency response of the reflection coefficient and all other factors vary far more

slowly than the resonance. This shows that we have proven that any resonator with a flat frequency response around the resonant frequency draws a circle in the complex reflection coefficient plane, which can be used to measure the properties of the resonance. Accordingly, if the frequency response is not flat, for example due to resonances in the coupling network, the resonance cannot be measured through this coupling network.

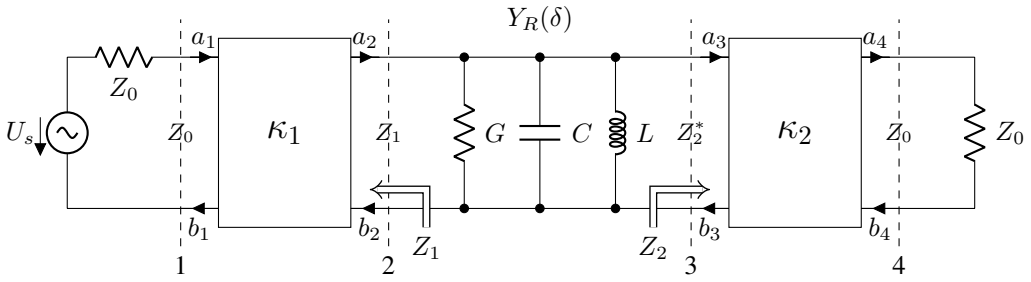

Figure 20: Transmission-type measurement

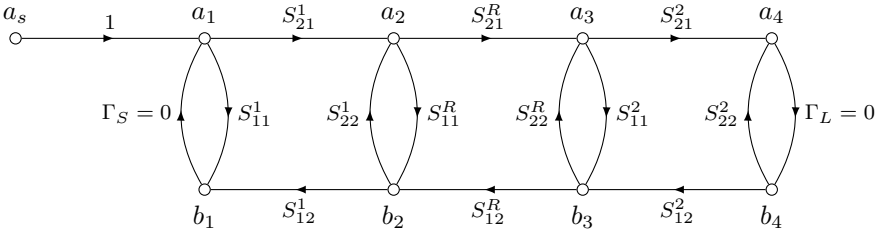

Figure 21: Signal flow graph of the measurement setup in Fig. 20.

B Transmission coefficient of a coupled resonant circuit

In chapter 4 we stated that any linear resonant circuit (RLC) draws a circle $(1 + jQ\delta)$ on a Smith chart and, therefore, has a very similar frequency response. To show that this statement applies to any resonant circuit, we start with a model of a transmission-type measurement shown in Fig. 20. The model in Fig. 20 features the transmission coefficient measurement of a linear resonant circuit with two coupling networks, κ_1 and κ_2, connected to port 1 and port 2 of the resonant circuit. At port 1 (ref. 2) we measure the output impedance Z_1 of the coupling network κ_1 and the source impedance Z_0 and at port 2 we measure the input impedance Z_2 of the coupling network κ_2 and the load Z_0. If we now choose the reference impedances at reference plane 2 and 3 cleverly, we can eliminate the output reflection coefficient of the source and the input reflection coefficient of the load. The same applies to reference plane 1 and 4, where the source and the load are matched to the reference impedance of the coupling networks. If we take a look at the signal flow graph of Fig. 21, it is obvious that if the output reflection coefficient at reference plane 2 is zero, then $S_{22}^1 = 0$ must apply to coupling network 1. The same applies to coupling network κ_2 and the input reflection coefficient at reference plane 3, where $S_{11}^2 = 0$. With these coefficients of the scattering matrices disappearing, we can conveniently simplify the signal flow graph of Fig. 21 and yield the following for the transmission coefficient

$$S_{41} = S_{21}^1 S_{21}^R S_{21}^2. \tag{29}$$

If we calculate the transmission coefficient S_{21}^R of the resonant circuit using the appropriate reference impedances Z_1 and Z_2^*, we get for

$$S_{21}^R = \sqrt{\frac{R_1}{R_2}} \frac{Y_1}{Y_1 + Y_2 + Y_R} = \sqrt{\frac{R_1}{R_2}} \frac{Y_1}{G_1 + jB_1 + G_2 + jB_2 + G(1 + jQ\delta)} \tag{30}$$

$$= \sqrt{\frac{R_1}{R_2}} \frac{Y_1}{(G + G_1 + G_2)(1 + jQ_L(\delta + \frac{B_1}{GQ_0} + \frac{B_2}{GQ_0}))}, \tag{31}$$

in which $R_1 = \mathrm{Re}\{Z_1\}, R_2 = \mathrm{Re}\{Z_2\}, Y_1 = 1/Z_1 = G_1 + jB_1, Y_2 = 1/Z_2 = G_2 + jB_2$ and Y_R is the impedance of the resonant circuit. Obviously, the unloaded resonator becomes loaded by the impedances Z_1 and Z_2, which change the detuning factor $\delta_L = -\frac{B_1}{GQ_0} - \frac{B_2}{GQ_0}$ and the quality factor $Q_L = Q_0/(1 + \frac{G_1}{G} + \frac{G_2}{G}) = Q_0/(1 + \kappa_1 + \kappa_2)$.

For the transmission coefficient S_{41} we can combine the results in (29) and (31) to the following expression

$$S_{41} = \sqrt{\frac{R_1}{R_2}} \frac{S_{21}^1 S_{21}^2 Y_1}{(G + G_1 + G_2)(1 + jQ_L(\delta + \frac{B_1}{GQ_0} + \frac{B_2}{GQ_0}))}. \tag{32}$$

Seeing that equation (32) also has a $(1 + jQ_L\delta)$-term in its denominator, we have shown that a resonant circuit coupled to any two coupling networks will also have a similar frequency response around its resonant frequency

provided that the frequency responses of the coupling networks are sufficiently flat in the frequency range around the resonant frequency.

References

[1] R. Clarke, Ed., *Guide to Characterisation of Dielectric Materials at RF Microwave Frequencies*. National Physical Laboratory, 2003. [Online]. Available: https://books.google.at/books?id=N4-lAAAACAAJ

[2] L. Chen, C. Ong, C. Neo, V. Varadan, and V. Varadan, *Microwave Electronics: Measurement and Materials Characterization*. Wiley, 2004. [Online]. Available: https://books.google.at/books?id=1vmUdUXlBNIC

[3] A. F. Horn, P. A. LaFrance, J. W. Reynolds, and J. Coonrod, "The influence of test method, conductor profile and substrate anisotropy on the permittivity values required for accurate modeling of high frequency planar circuits," *Circuit World*, vol. 38, no. 4, pp. 219–231, Novemeber 2012.

[4] *Stripline Test for Permittivity and Loss Tangent (Dielectric Constant and Dissipation Factor) at X-Band*, IPC - Association Connecting Electronics Industries TM-650 Test Methods Manual 2.5.5.5, Rev. C, March 1998.

[5] M. D. Janezic, N. Paulter, and J. Blendell, "Dielectric and conductor-loss characterization and measurements on electronic packaging materials," *NIST Technical note*, vol. 1520, 2001.

[6] *Test methods for electrical materials, printed boards and other interconnection structures and assemblies - Part 2-721: Test methods for materials for interconnection structures - Measurement of relative permittivity and loss tangent for copper clad laminate at microwave frequency using a split post dielectric resonator*, IEC International Standard 61 189-2-721:2015, March 2016.

[7] M. D. Janezic and J. Krupka, "Split-post and split-cylinder resonator techniques: A comparison of complex permittivity measurement of dielectric substrates," *Journal of Microelectronics and Electronic Packaging*, vol. 6, no. 2, pp. 97–100, 2009.

[8] J. Krupka, R. G. Geyer, J. Baker-Jarvis, and J. Ceremuga, "Measurements of the complex permittivity of microwave circuit board substrates using split dielectric resonator and reentrant cavity techniques," in *Dielectric Materials, Measurements and Applications, Seventh International Conference on (Conf. Publ. No. 430)*. IET, 1996, pp. 21–24.

[9] P. J. Petersan and S. M. Anlage, "Measurement of resonant frequency and quality factor of microwave resonators: Comparison of methods," *Journal of applied physics*, vol. 84, no. 6, pp. 3392–3402, 1998.

[10] P. Bevington and D. Robinson, *Data Reduction and Error Analysis for the Physical Sciences*, ser. McGraw-Hill Higher Education. McGraw-Hill, 2003. [Online]. Available: https://books.google.at/books?id=JYaZPwAACAAJ

[11] K. J. Coakley, J. D. Splett, M. D. Janezic, and R. F. Kaiser, "Estimation of q-factors and resonant frequencies," *IEEE Transactions on Microwave Theory and Techniques*, vol. 51, no. 3, pp. 862–868, Mar 2003.

[12] M. D. Janezic, "Nondestructive relative permittivity and loss tangent measurements using a split-cylinder resonator," Ph.D. dissertation, University of Colorado, 2003.

[13] A. J. Estin and M. D. Janezic, "Improvements in dielectric measurements with a resonant cavity," in *Instrumentation and Measurement Technology Conference, 1991. IMTC-91. Conference Record., 8th IEEE*. IEEE, 1991, pp. 573–579.

[14] P. G. Bartley and S. B. Begley, "Quality factor determination of resonant structures," in *2006 IEEE Instrumentation and Measurement Technology Conference Proceedings*. IEEE, 2006, pp. 312–316.

[15] D. Pozar, *Microwave Engineering, 4th Edition*. Wiley, 2011. [Online]. Available: https://books.google.at/books?id=JegbAAAAQBAJ

[16] C. Montgomery, R. Dicke, and E. Purcell, *Principles of Microwave Circuits*, ser. Electromagnetics and Radar Series. Institution of Engineering & Technology, 1948. [Online]. Available: https://books.google.sh/books?id=Sex_282iULMC